INFECTION AND IMMUNITY, Aug. 1999, p. 4201–4207 Vol. 67, No. 8
0019-9567/99/$04.00+0

Dynamics of Actin-Based Movement by *Rickettsia rickettsii* in Vero Cells

ROBERT A. HEINZEN,* SCOTT S. GRIESHABER, LEVI S. VAN KIRK, AND CLINTON J. DEVIN

Department of Molecular Biology, University of Wyoming, Laramie, Wyoming 82071-3944

Received 9 February 1999/Returned for modification 24 March 1999/Accepted 20 May 1999

Actin-based motility (ABM) is a virulence mechanism exploited by invasive bacterial pathogens in the genera *Listeria*, *Shigella*, and *Rickettsia*. Due to experimental constraints imposed by the lack of genetic tools and their obligate intracellular nature, little is known about rickettsial ABM relative to *Listeria* and *Shigella* ABM systems. In this study, we directly compared the dynamics and behavior of ABM of *Rickettsia rickettsii* and *Listeria monocytogenes*. A time-lapse video of moving intracellular bacteria was obtained by laser-scanning confocal microscopy of infected Vero cells synthesizing β-actin coupled to green fluorescent protein (GFP). Analysis of time-lapse images demonstrated that *R. rickettsii* organisms move through the cell cytoplasm at an average rate of 4.8 ± 0.6 μm/min (mean ± standard deviation). This speed was 2.5 times slower than that of *L. monocytogenes*, which moved at an average rate of 12.0 ± 3.1 μm/min. Although rickettsiae moved more slowly, the actin filaments comprising the actin comet tail were significantly more stable, with an average half-life approximately three times that of *L. monocytogenes* (100.6 ± 19.2 s versus 33.0 ± 7.6 s, respectively). The actin tail associated with intracytoplasmic rickettsiae remained stationary in the cytoplasm as the organism moved forward. In contrast, actin tails of rickettsiae trapped within the nucleus displayed dramatic movements. The observed phenotypic differences between the ABM of *Listeria* and *Rickettsia* may indicate fundamental differences in the mechanisms of actin recruitment and polymerization.

Rickettsia rickettsii is the bacterial agent of Rocky Mountain spotted fever (51). Because of experimental limitations imposed by the obligate intracellular nature of the organism, little is known about specific virulence determinants utilized by this and other *Rickettsia* spp. Insight into the virulence of spotted fever group rickettsiae, such as *R. rickettsii*, was achieved with the discovery that these organisms utilize an intracellular actin-based motility (ABM) system to promote direct cell-to-cell spread (17, 27, 42). This mechanism of pathogenesis is also exploited by the facultative intracellular bacteria *Listeria monocytogenes* and *Shigella flexneri* (reviewed in references 8 and 43). By using the propulsive force supplied by parasite-directed polymerization of host cell actin, motile bacteria move into pseudopodia that can be subsequently engulfed by neighboring cells. Escape from the double membrane vacuole allows infection of the new cytoplasm (46). The ability of spotted fever group rickettsiae to spread via ABM within the endothelium (the target host tissue of rickettsia) by directly passing from one cell to another allows evasion of the host humoral immune response, minimizes exposure to cell-impermeant antibiotics, and maintains rickettsiae within their required intracellular niche.

Many of the cellular events and proteins necessary for ABM by *Shigella* and *Listeria* have been defined. Elegant genetic studies have identified the surface proteins ActA and IcsA (VirG) as necessary and sufficient for ABM by *L. monocytogenes* and *S. flexneri*, respectively (14, 20, 37, 50). Both proteins are asymmetrically localized on the bacterial outer surface in the vicinity of the growing actin tail (13, 19). Despite similar roles in ABM, these proteins are not homologous (2, 11, 18, 23). Assembly of actin tails requires recruitment of host factors by ActA and IcsA that control dynamic actin processes. Both proteins interact with vasodilator-stimulated phosphoprotein (VASP). VASP is a substrate for cyclic AMP- and cyclic GMP-dependent protein kinases and is generally localized to focal adhesions and areas of high actin turnover (33). VASP directly binds a proline-rich motif of ActA (6, 28). Conversely, IcsA, via its glycine-rich repeats, binds the 90-kDa head fragment of vinculin, (21, 41), a protein that normally links F-actin (filamentous actin) to plasma membrane integrins at focal adhesion points (12). Vinculin contains an ActA-like proline-rich motif that serves as a VASP binding site (4, 34). In both situations, VASP serves as ligand for profilin, an actin monomer sequestering protein that promotes actin assembly in free barbed ends of actin filaments (32, 33). The VASP-profilin-actin complex is thought to provide a local pool of polymerization-competent actin monomers to the unipolar polymerization zone of the bacterium (45). In addition to VASP, the N terminus of ActA has recently been shown to associate with actin-related protein (ARP) complex 2/3, a seven-protein complex that may confer nucleating activity for actin filamentation (48–50). *Shigella* actin assembly and movement require the additional recruitment by IcsA of neural Wiskott-Aldrich syndrome protein (N-WASP), a protein involved in filopodia production (26, 40).

Rickettsial protein synthesis is required for ABM, although the nature of this protein(s) and the identity of host factors necessary for rickettsial ABM remain to be defined. However, some of the temporal events in rickettsial ABM have been elucidated (17). Escape from the nascent endocytic vacuole occurs as early as 15 min postinfection. Rickettsiae then become surrounded by an intensely stained actin cloud, as demonstrated by fluorescent phalloidin staining. This cloud is reorganized into the typical polar actin "comet tail," observed as early as 30 min postinfection. F-actin tails grow considerably longer than those of *Listeria* and *Shigella*, often exceeding 30 μm in length. Transmission electron microscopy depicts *R. rickettsii* with a polar association of long, parallel actin filaments that appear to be periodically cross-linked. Scanning

* Corresponding author. Mailing address: Department of Molecular Biology, University of Wyoming, Laramie, WY 82071-3944. Phone: (307) 766-5458. Fax: (307) 766-3875. E-mail: rheinzen@uwyo.edu.

electron microscopy of infected Vero cells depicts rickettsiae within short pseudopodia (~5 μm long) (16a). These parasite-containing pseudopodia can presumably be internalized by adjacent cells, as has been documented for *Listeria* and *Shigella* (31, 46). Dissolution of the double membrane surrounding the bacterium would then allow the organism access to the cytoplasm of the newly encountered cell. Alternatively, organisms can be released directly into the extracellular space, and this release can be inhibited by cytocholasin D, a powerful inhibitor of actin polymerization (17).

The dynamics of *S. flexneri* and *L. monocytogenes* ABM have been extensively studied with video microscopy of movements within live cells and cell lysates (9, 14, 36, 45). In this study, we have documented for the first time ABM by *R. rickettsii* and compared it directly to that of *L. monocytogenes*. Dynamics of actin-based movement were evaluated by time-lapse microscopy of bacteria moving in Vero cells synthesizing a β-actin–green fluorescent protein (GFP) chimera. Significant differences in the dynamics and behavior of *R. rickettsii* ABM were observed compared with those of the ABM of *L. monocytogenes*.

MATERIALS AND METHODS

Organisms. *R. rickettsii* (HLP strain) was propagated in African green monkey kidney (Vero) fibroblasts (CCL-81; American Type Culture Collection), and cells were purified by Renografin density gradient centrifugation as previously described (16). *L. monocytogenes* 1043S was a generous gift of Dan Portnoy, University of California at Berkley, and was cultivated overnight in 3.7% brain heart infusion (BHI) broth (Difco Laboratories, Detroit, Mich.). COS-7 cells (African green monkey kidney fibroblasts [CRL-1651; American Type Culture Collection]) were used as a control in transfection experiments.

Construction of GFP-actin. The human β-actin gene was amplified from a HeLa cell cDNA library (Stratagene, La Jolla, Calif.) by PCR. The 5′ oligonucleotide GAAGATCTATGGATGATGATATCGCCG contains a *Bgl*II site and the β-actin ATG start codon. The 3′ oligonucleotide CGGAATTCCTAGGAA GCATTTGCGGTCG contains an *Eco*RI site and the β-actin stop codon. The resulting 1,143-bp PCR product was digested with *Bgl*II and *Eco*RI, and the β-actin reading frame was cloned in frame with the 5′ end of *gfp* carried by pEGFP-C1 (Clontech Laboratories, Inc., Palo Alto, Calif.). Nucleotide sequencing of the region encoding the GFP-actin fusion junction of the resulting clone (pEFGP-C1/actin) confirmed the cloning procedure.

Infection and transfection of Vero cells. Twelve- or 35-millimeter glass coverslips, in 24- or 6-well plates, respectively, were seeded with Vero cells to semiconfluency and cultivated overnight at 37°C in M199 medium (Life Technologies, Grand Island, N.Y.) supplemented with 10% fetal bovine serum (FBS) (Life Technologies) and 20 μg of gentamicin per ml (Life Technologies). Rickettsiae suspended in 3.7% BHI broth (Difco Laboratories) were used to infect monolayers at a multiplicity of infection of 0.1 to 1.0 for 45 min. The inoculum was removed, the cells were washed once, M199 medium supplemented with 2% FBS was added, and incubation continued at 34°C. For infection of Vero cells with *L. monocytogenes*, an overnight culture of *Listeria* in BHI broth was pelleted, washed once, and suspended in twice the culture volume of Hank's buffered saline solution (HBSS) (Life Technologies). Two hundred to 300 μl of suspended bacteria was added to each tissue culture plate well, and the plates were then incubated for 1 h at room temperature. Vero cells were then washed three times with HBSS, and M199 medium supplemented with 2% FBS and 20 μg of gentamicin sulfate per ml was added to culture wells.

Transfections with pEGFP-C1/actin were conducted on semiconfluent Vero cell monolayers cultivated on 35-mm-diameter coverslips by using LipofectAMINE and methods suggested by the supplier (Life Technologies). Due to the slow growth rate of rickettsiae, cells were infected with *R. rickettsii* for 2 days prior to transfection. Rickettsial infection and expression of GFP-actin were then allowed to proceed for an additional 1 to 2 days before microscopy. Vero cells were infected with *L. monocytogenes* 1 day after transfection, and the infection was allowed to proceed for 24 to 36 h before microscopy.

Immunofluorescence staining. All fixation and staining procedures were carried out at room temperature. Infected cells on coverslips were fixed and permeabilized as previously described (17). Fixed cells were then washed three times in 25 mM sodium phosphate–150 mM sodium chloride (pH 7.4) containing 0.5% bovine serum albumin. *R. rickettsii* cells were labeled by indirect immunofluorescence with the monoclonal antibody 13-2 directed against the rOmpB protein (1) and an anti-mouse immunoglobulin G (IgG)–Texas red conjugate (Jackson ImmunoResearch Laboratories, Inc., West Grove, Pa.). *L. monocytogenes* cells were labeled with rabbit anti-*Listeria* serum (Biodesign International, Kennebunk, Maine) and an anti-rabbit IgG–rhodamine conjugate (Pierce, Rockford, Ill.). Coverslips were mounted onto glass slides with Vectashield mounting medium (Vector Laboratories, Inc., Burlingame, Calif.).

Laser-scanning confocal microscopy. Laser-scanning confocal microscopy of both fixed and live infected cells was conducted with a Leica confocal microscope equipped with krypton-argon laser illuminators. Collected images were processed with Adobe Photoshop 3.0 and NIH Image 1.61. Live cells were visualized by placing the coverslip cell side down onto a small drop of medium on a glass slide. Vero cells synthesizing GFP-actin that were lightly infected with 1 to 20 organisms having clearly visible GFP-actin tails were chosen for time-lapse microscopy. Time-lapse video microscopy was conducted on 3 separate days with Vero cells that were infected with either organism and cultivated under similar conditions. Images were collected at 21-s intervals and were assembled into video stacks by using NIH Image. Bacteria in the archived digital video having easily distinguishable actin tails were randomly chosen for tracking. They were tracked until they moved out of the confocal plane of focus, which ranged from 84 to 240 s. The rate of bacterial movement was measured by tracking the pixel position of the actin-polymerizing end of individual bacteria over time and is expressed as micrometers per minute. The F-actin half-life was calculated by measuring the pixel density of GFP-actin fluorescence every 21 s in a fixed area over the stationary actin tail. Background fluorescence intensity, as determined by measuring the fluorescence emission of an area of similar size next to the actin tail, was subtracted from each time point.

RESULTS

Expression of GFP-actin. GFP-actin chimeras have been successfully employed in studies of dynamic actin processes of yeast, *Dictyostelium*, and mammalian cells (24). To allow real-time visualization of rickettsial ABM, we constructed the plasmid pEGFP-C1/actin which directs the synthesis of GFP fused to the N terminus of human β-actin. Functional expression of the approximately 70-kDa GFP-actin fusion protein was evident in transfected Cos7 cells where the protein chimera incorporated into prominent F-actin stress fibers (Fig. 1A). These GFP-actin-containing F-actin structures colocalized with F-actin fluorescently stained with rhodamine-phalloidin. A similar stress fiber incorporation profile was observed in Vero cells (data not shown). To determine whether GFP-actin was incorporated into rickettsial actin tails, Vero cells infected with *R. rickettsii* were transfected with pEGFP-C1/actin and subsequently visualized by confocal microscopy (Fig. 1B). Actin tails containing GFP-actin were indistinguishable in morphology and length from those observed by rhodamine-phalloidin staining. A similar result was obtained for *L. monocytogenes* (Fig. 1C).

Dynamics of rickettsial ABM. Incorporation of GFP-actin into rickettsial and listerial actin tails allowed a comparative analysis of the dynamics of ABM by each organism. Time-lapse observation of ABM was conducted by using laser-scanning confocal fluorescence microscopy as described in Materials and Methods. As depicted in Fig. 2, sequential confocal images of live cells collected at 21-s intervals clearly demonstrate the forward movement of both organisms. The nonfluorescent bacteria are juxtaposed with the highly fluorescing front of the F-actin tail that has a cup-shaped appearance. By tracking the position of the front of the actin tail over time, we determined that *R. rickettsii* organisms move through the cell cytoplasm at a mean rate of 4.8 ± 0.6 μm/min (mean ± standard deviation [SD]; $n = 28$). As indicated by the low SD, the rate of movement was very consistent between rickettsiae. The rate of rickettsial ABM was 2.5 times slower than that measured for *L. monocytogenes*, which moved at a mean rate of 12.0 ± 3.1 μm/min (mean ± SD; $n = 23$).

Close examination of the time-lapse video revealed many phenotypic differences in actin tail structure and movement patterns between *L. monocytogenes* and *R. rickettsii*. *Listeria* were frequently observed turning in tight circles, and organisms tracking in straight paths often made sudden changes in the direction of movement. In contrast, rickettsiae tended to move in much straighter paths, with rapid changes in direction

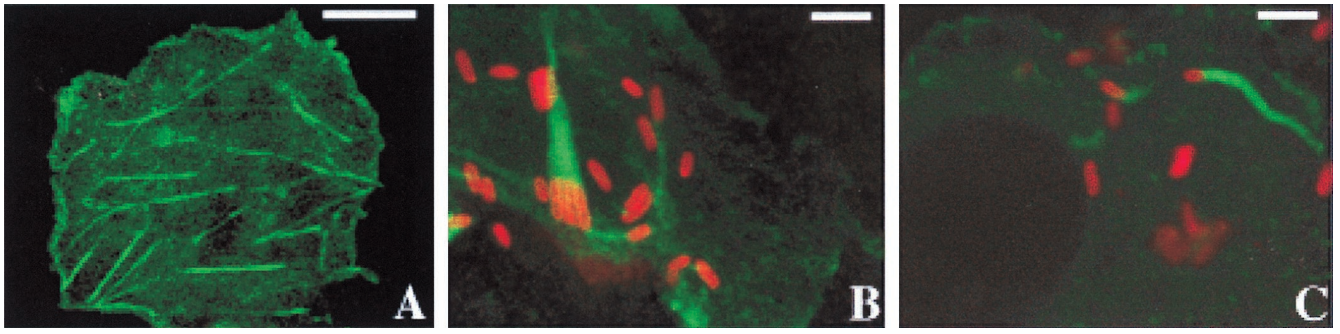

FIG. 1. Incorporation of GFP-actin into COS-7 cell stress fibers and actin tails of *R. rickettsii* and *Listeria monocytogenes* within Vero cells. Mammalian cell cultures were transfected with the plasmid pEGFP-C1/actin encoding GFP–β-actin and infected with either *L. monocytogenes* or *R. rickettsii*. Transfected COS-7 cells were fixed and viewed without subsequent staining. Infected Vero cells were fixed and permeabilized, and intracellular bacteria were stained by indirect immunofluorescence with the second antibody conjugated to rhodamine (red). (A) Incorporation of GFP-actin (green) into stress fibers of COS-7 cells. (B) Incorporation of GFP-actin into *R. rickettsii* actin tails. Note the cluster of organisms undergoing binary fission with one large polar actin tail. (C) Incorporation of GFP-actin into *L. monocytogenes* actin tails. Bars: panel A, 15 μm; panel B, 2 μm; panel C, 3 μm.

occurring only when coming in contact with cellular structures that impeded forward movement, such as the plasma membrane. In a typical cell, the percentage of stationary *Listeria* was also greater than that of *Rickettsia*. Moreover, stationary rickettsiae were usually surrounded by a uniform actin coat, whereas the actin coat of stationary *Listeria* was generally concentrated at one or both poles of the bacterium (36). (Quicktime movies of time-lapse video can be viewed at the URL addresses given in references 3a and 3b.)

Structural differences between the GFP-actin-containing tails of *Listeria* and *Rickettsia* were also clearly apparent. For example, listerial tails were shorter, with a more uniform gradient of fluorescence beginning at the bacterium-tail interface and extending outward. Rickettsial tails often appeared as mul-

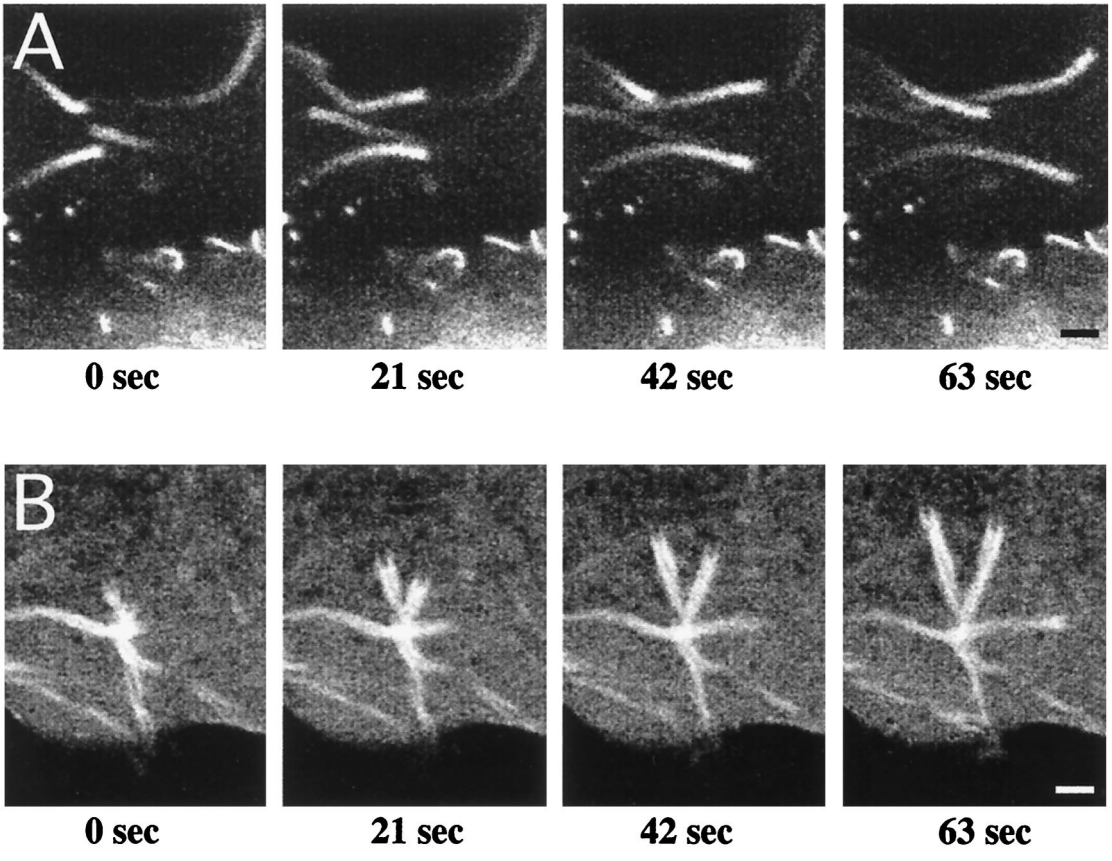

FIG. 2. Time-lapse video fluorescence microscopy of *Listeria* and *Rickettsia* ABM. Vero cells were transfected with the plasmid pEGFP-C1/actin encoding GFP–β-actin and infected with either *L. monocytogenes* or *R. rickettsii*. Laser-scanning confocal fluorescence microscopy was conducted with live cells, and images were collected every 21 s. (A) Actin-based movement of *Listeria*. The average rate of movement was 12 μm/min (n = 23). (B) Actin-based movement of *Rickettsia*. The average rate of movement was 4.8 μm/min (n = 28). Bars, 2.5 μm.

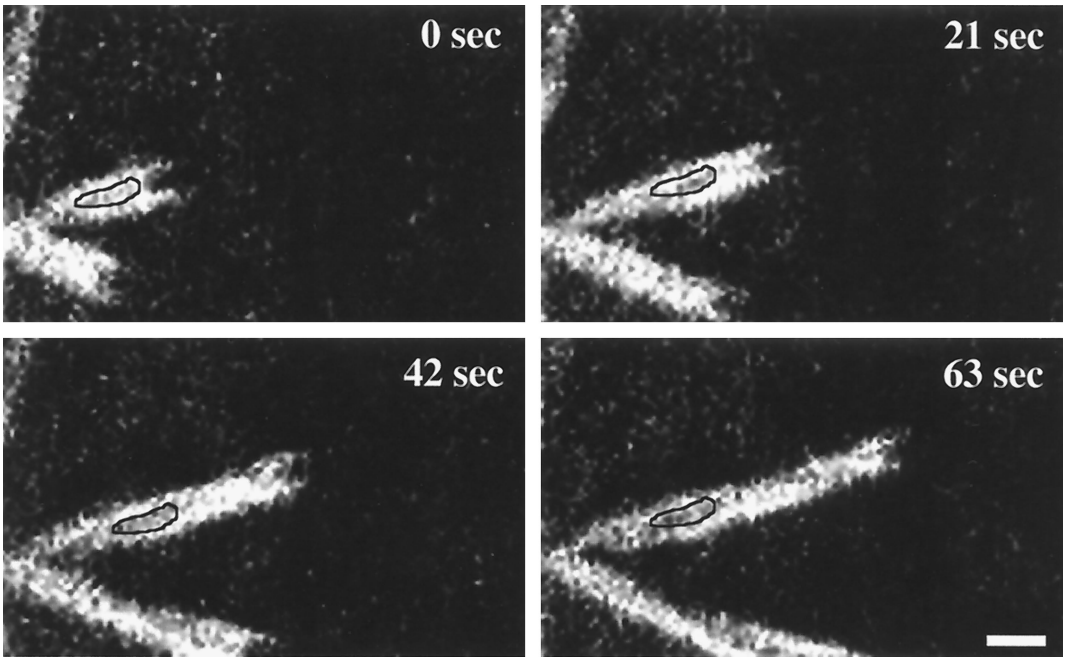

FIG. 3. Time-lapse video fluorescence microscopy of *Rickettsia* ABM documenting the stationary nature of intracytoplasmic rickettsial actin tails. Vero cells were transfected with the plasmid pEGFP-C1/actin encoding GFP–β-actin and infected with *R. rickettsii*. Laser-scanning confocal fluorescence microscopy was conducted with live cells. Images were collected every 21 s. Gaps (outlined areas) that arise because of the helical twisting of the bifurcated rickettsial tail appendage remain stationary as the bacterium moves forward. Bar, 2 μm.

tiple bundles of actin filaments, wrapping around each other in a helical fashion to give rise to nonfluorescent gaps in the tail structure. This tail structure is somewhat evident in Fig. 2B and was observed in our previous study (17). One full helical turn of each F-actin strand was observed roughly every 6 μm, leaving nonfluorescent gaps of approximately 3 μm in the actin tail. Close observation of sequential images indicated that the gaps are fixed in space over time (Fig. 3). This observation implies that the tail remains stationary as the rickettsia moves forward through the cytosol. The stationary behavior of the rickettsial actin tail would be consistent with actin tail formation and movement by *L. monocytogenes* (9, 36, 44) and *S. flexneri* (14).

Tail F-actin half-life. The stationary property of actin tails of cytoplasmic rickettsiae allowed a simple determination of the relative half-life of actin filaments comprising the tail. The pixel density of GFP-actin fluorescence was calculated every 21 s in a fixed area over the stationary actin tail with the initial measurement taken immediately adjacent to the bacterium. Background fluorescence intensity was determined by measuring the fluorescence emission of an area of similar size next to the actin tail and was subtracted from each time point. Repeated illumination of GFP-actin revealed no obvious photobleaching, an established property of GFP (7). The half-life of F-actin comprising rickettsial tails (100.6 ± 19.2 [mean ± SD; $n = 14$]) was approximately threefold longer than that of listerial tails (33.0 ± 7.6 s [mean ± SD; $n = 17$]) (Fig. 4). Measurements throughout the rickettsial tail revealed nearly identical F-actin half-lives.

Intranuclear movements. Spotted fever group rickettsiae have the unusual ability to penetrate and replicate within the nucleus (47). In cells producing GFP-actin, intranuclear rickettsia were often observed with actin tails (Fig. 5). These organisms were frequently clumped together and associated with one large, highly fluorescing actin tail that often grew to great lengths, occasionally winding throughout the nucleus. In contrast to the stationary behavior of tails of cytoplasmic rickettsiae, tails of intranuclear rickettsiae underwent dramatic movements when observed by time-lapse microscopy (Fig. 5). Obvious force was imposed upon the nuclear membrane by both the clump of rickettsiae at the head of the tail and distal portions of the actin tail, distorting the membrane. This particular cell was observed for 10 min, during which time, the clump of rickettsiae did not move forward. Release of rickettsiae from the nucleus was never observed.

DISCUSSION

In this report, we describe for the first time the dynamics of rickettsial ABM. As a fluorescent marker of ABM within live cells, we employed a GFP-actin chimera. This composite protein exhibited a phenotype similar to that of native β-actin by incorporating into actin the stress fibers and actin tails of *R. rickettsii* and *L. monocytogenes*. Transient expression of GFP-actin is a simple method with which to visualize ABM and obviates the need for more technically challenging protocols, such as microinjection of fluorescently tagged actin into individual cells (9, 36, 44). Our calculated average speed of *Listeria* actin-based movement (12 μm/min) is in excellent agreement with previously reported rates (9, 36, 38, 44, 45). Moreover, the calculated half-life of listerial tail actin filaments is consistent with measurements by Theriot et al. (44), who calculated an F-actin half-life of 33 s. These data validate the use of GFP-actin in the study of bacterial ABM. While intracellular movements of *Shigella* and *Listeria* can be directly visualized by phase-contrast light microscopy, the smaller size of rickettsia has made it difficult to document rickettsial movement in a similar fashion.

The rates of movement of different rickettsiae were remarkably consistent, with an average speed of 4.8 μm/min. This is 2.5 times slower than *Listeria* ABM. We also observed much

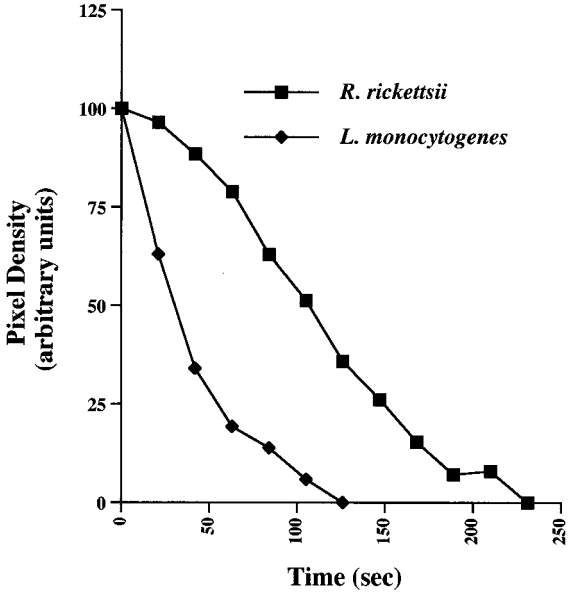

FIG. 4. Half-life of F-actin comprising the rickettsial actin tail and comparison with that of *L. monocytogenes*. A representative fluorescence intensity profile of a single actin tail from each organism is shown. Fluorescence intensity profiles were determined by measuring the pixel density of GFP-actin fluorescence emission every 21 s in a fixed area over the stationary actin tail. Background fluorescence intensity, as determined by measuring the fluorescence emission of an area of similar size next to the actin tail, was subtracted from each time point. These examples are representative of 14 and 17 tails of *R. rickettsii* and *L. monocytogenes*, respectively. With each organism, the shape of the intensity profile approximates exponential decay.

more variation in the rate of listerial ABM, which is consistent with published observations (9, 36, 38, 44, 45). Among other factors, the variability in speed has been attributed to encounters with stress fibers and other structural elements (9). The smaller size of *Rickettsia* (~0.3 by 1 μm) relative to *Listeria* (~0.5 by 2 μm) may mean that rickettsiae have fewer collisions with intracellular structures, resulting in more uniform rates of movement. The fact that rickettsiae move in straighter paths than *Listeria* may permit more accurate measurements of the path distances. A study by Theriot et al. (44) concluded that *Listeria* cells with the longest tails move the fastest. We were unable to determine if such a correlation exists for rickettsiae, because the bacteria moved in and out of the confocal focus plane during image capture. Thus, total tail lengths could not be reliably measured.

VASP is an accelerator of listerial ABM and binds a proline-rich motif in the central region of *Listeria* ActA (6, 28). Deletion of this motif eliminates VASP binding and slows the rate of *Listeria* ABM by two- to threefold to about 5 μm/min (22, 38), approximating the rate of rickettsial ABM. In contrast to *Listeria*, in which VASP is localized to the polymerizing end of the bacterium (6), rickettsial VASP is diffusely dispersed throughout the actin tail and does not display concentrated unipolar localization with the organism (unpublished observations). Whether VASP serves a functional role in facilitating rickettsial ABM by recruiting profilin-actin complexes to the polymerization zone has yet to be determined. The fact that rickettsiae move at approximately the same rate as *Listeria* ActA mutants deficient for VASP recruitment may suggest that rickettsiae do not utilize VASP as an accelerator of ABM.

Analysis of individual rickettsial F-actin tails revealed a gradient of fluorescence intensity, from the bacterium-tail interface to the end of the tail, that approximates exponential decay (data not shown). Myosin S1 subfragment decoration shows the fast-growing barbed ends of individual actin filaments of the tail oriented toward the rickettsial surface (unpublished observations). Collectively, these data support the notion that, like *Listeria*, the rate of incorporation of actin monomers at the rickettsia-tail interface approximates the rate of bacterial movement and that the rickettsial F-actin tail represents a

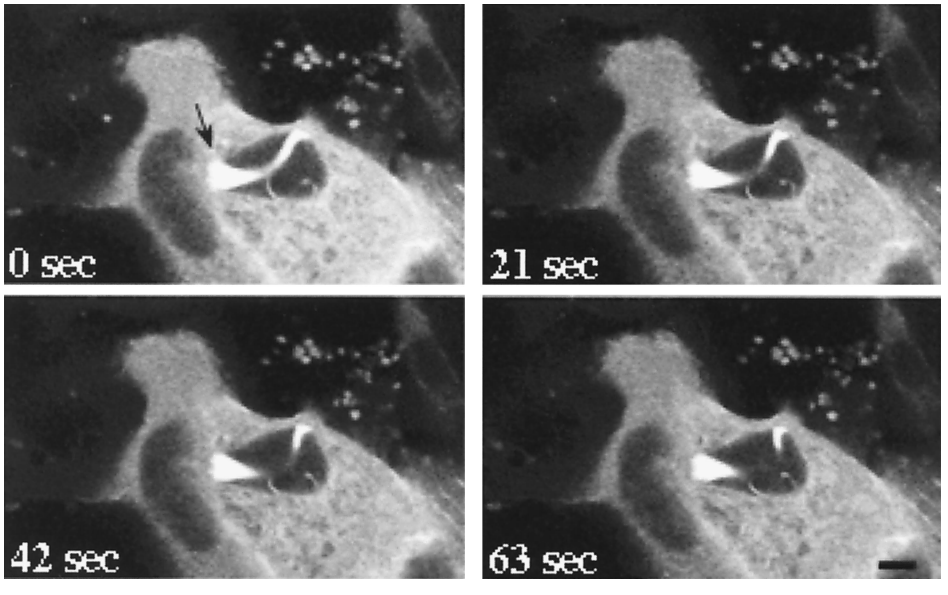

FIG. 5. Time-lapse video fluorescence microscopy of intranuclear *R. rickettsii*. Vero cells were transfected with the plasmid pEGFP-C1/actin encoding a GFP–β-actin chimera. Cells were subsequently infected with *R. rickettsii*. Laser-scanning confocal fluorescence microscopy was conducted with live cells, and images were collected every 21 s. Two adjacent transfected cells are depicted in this micrograph. The strongly fluorescing cytoplasm surrounds the darker, oval-shaped nucleus. This 63-s sequence demonstrates force being exerted against the nuclear envelope by both the cluster of rickettsiae at the head of the actin tail (arrow) and an interior portion of the actin tail. Dramatic movement of the middle of the actin tail is obvious, with no forward movement of rickettsiae observed. The end of the actin tail is visible at the bottom right of the nucleus. Bar, 5 μm.

structural scaffold to which new building blocks in the form of G-actin, or possibly small F-actin units, are continually added at the tail-bacterium interface, thereby pushing the organism forward through the viscous cytosol (9, 36, 44).

The distinct actin tail bundles that articulate with the rickettsial surface suggest that the pole of the bacterium harbors multiple asymmetrically opposed polymerization zones (17). Asymmetric assembly of actin bundles could result in the helical twisting of the actin tail and implies that the organism rotates as it moves forward. Considering that the periodicity of the helical turns is roughly 6 μm/turn and that rickettsiae move at approximately 5 μm/min, one can speculate that the organism rotates approximately once every minute.

The F-actin of rickettsial actin tails was about three times more stable than that of listerial tails, having an average half-life of 100 s. These data are consistent with our previous observation that rickettsial tails are more stable than listerial tails following treatment with cytocholasin D, a fungal toxin that caps the barbed ends of F-actin and results in net depolymerization (3, 17, 36). The greater stability of rickettsial tails relative to listerial tails may reflect differential activities of host proteins involved in F-actin severing or the off rate of actin monomers. Actin depolymerizing factor (ADF)/cofilin, is known to affect actin filament turnover in *Listeria* tails by one or both of these functions (5, 25, 35). Moreover, F-actin bundling proteins, such as α-actinin, play critical roles in *Listeria* actin tail stability (10). Future studies should reveal whether these proteins serve similar roles in rickettsial F-actin tail turnover.

The mechanism of rickettsial entry into the nucleus is unknown. Some authors have suggested that rickettsiae are simply trapped in this compartment as a consequence of nuclear division (47). A more likely scenario is that rickettsiae directly penetrate the nuclear membrane, aided by the propulsive force of actin tail assembly and, possibly, phospholipase activity (51). We have observed cytoplasmic organisms perturbing the nuclear envelope that appear to be in the process of penetration (unpublished observations). Nuclear pores, which can dilate to 26 nm with the appropriate signal, are too small to allow transit of the much larger rickettsiae (29).

Previous studies have reported that intranuclear rickettsiae lack actin tails (17, 42). Here we clearly demonstrate the assembly of actin tail appendages by rickettsiae within this compartment by using laser-scanning confocal microscopy. The epifluorescence microscopy used in previous studies may have been inadequate to resolve the actin tails of intranuclear rickettsiae, which tend to form high-density microcolonies in the nucleus. The complement of actin binding and accessory proteins within this compartment is unknown, but those necessary for rickettsial ABM and tail formation are obviously present. Along with actin, the nucleus contains at least 450 other nonhistone proteins (15, 30). Nuclear pores allow the free transit of molecules of approximately ≤70 kDa (39). GFP-actin, having a molecular weight of approximately 70,000, equilibrated with the nuclear compartment, albeit at a lower concentration than the cytosol, based on GFP fluorescence intensity. Some stable host factors necessary for ABM and bound to the surface of rickettsia may be carried in by penetrating organisms. The observation that tails of intranuclear rickettsiae grow exceedingly long may indicate the lack of depolymerizing factors in the nucleus. Obvious physical force was exerted upon the nuclear membrane by both the rickettsial head and distal portions of the actin tail, distorting the membrane, and forward movement of rickettsiae was impeded. Moreover, pronounced movement of the actin tail was observed in contrast to the stationary nature of cytoplasmic tails. This movement may result from treadmilling of actin monomers comprising tail filaments in association with rickettsiae that are unable to move forward (3). The clumping of intranuclear rickettsiae may be a manifestation of the spatial constraints imposed on organisms within this compartment that result in the cross-linking of F-actin between multiple tails.

The significant phenotypic differences observed between *R. rickettsii* and *L. monocytogenes* indicate fundamental differences in the mechanism of ABM. GFP-tagged actin provides a model system with which to more clearly define the mechanics of rickettsial ABM. The results of these experiments will assist in development of a mechanistic model for rickettsial actin-based movement and will hopefully lead to the elucidation of the rickettsial protein(s) essential for this process.

ACKNOWLEDGMENTS

We thank Ted Hackstadt, Shelly Robertson, and Scott Boitano for critical review of the manuscript.

This work was supported by National Institutes of Health grant AI-43502-01 (R.A.H.).

REFERENCES

1. **Anacker, R. L., R. E. Mann, and C. Gonzales.** 1987. Reactivity of monoclonal antibodies to *Rickettsia rickettsii* with spotted fever and typhus group rickettsiae. J. Clin. Microbiol. **25:**167–171.
2. **Bernardini, M. L., J. Mounier, H. d'Hautevile, M. Coquis-Rondon, and P. J. Sansonetti.** 1989. Identification of *icsA*, a plasmid locus of *Shigella flexneri* that governs bacterial intra- and intercellular spread through interaction with F-actin. Proc. Natl. Acad. Sci. USA **86:**3867–3871.
3. **Bershadsky, A. D., and J. M. Vasiliev (ed.).** 1988. Cytoskeleton. Plenum Publishing Corp., New York, N.Y.

3a. **Boitano, S.** 9 February 1999, posting date. [Online.] http://august.uwyo.edu/boitanolab/actin240.mov. [8 June 1999, last date accessed.]

3b. **Boitano, S.** 9 February 1999, posting date. [Online.] http://august.uwyo.edu/boitanolab/actin480.mov. [8 June 1999, last date accessed.]

4. **Brindle, N. P., M. R. Holt, J. E. Davies, C. J. Price, and D. R. Critchley.** 1996. The focal-adhesion vasodilator-stimulated phosphoprotein (VASP) binds to the proline-rich domain in vinculin. Biochem. J. **318:**753–757.
5. **Carlier, M. F., V. Laurent, J. Santolini, R. Melki, D. Didry, G. X. Xia, Y. Hong, N. H. Chua, and D. Pantaloni.** 1997. Actin depolymerizing factor (ADF/cofilin) enhances the rate of filament turnover: implication in actin-based motility. J. Cell Biol. **136:**1307–1322.
6. **Chakraborty, T., F. Ebel, E. Domann, K. Niebuhr, B. Gerstel, S. Pistor, C. J. Temm-Grove, B. M. Jockusch, M. Reinhard, U. Walter, and J. Wehland.** 1995. A focal adhesion factor directly linking intracellularly motile *Listeria monocytogenes* and *Listeria ivanovii* to the actin-based cytoskeleton of mammalian cells. EMBO J. **14:**1314–1321.
7. **Chalfie, M., Y. Tu, G. Euskirchen, W. W. Ward, and D. C. Prasher.** 1994. Green fluorescent protein as a marker for gene expression. Science **263:**802–805.
8. **Cossart, P.** 1997. Subversion of the mammalian cell cytoskeleton by invasive bacteria. J. Clin. Investig. **99:**2307–2311.
9. **Dabiri, G. A., J. M. Sanger, D. A. Portnoy, and F. S. Southwick.** 1990. *Listeria monocytogenes* moves rapidly through the host-cell cytoplasm by inducing directional actin assembly. Proc. Natl. Acad. Sci. USA **87:**6068–6072.
10. **Dold, F. G., J. M. Sanger, and J. W. Sanger.** 1994. Intact alpha-actinin molecules are needed for both the assembly of actin into the tails and the locomotion of *Listeria monocytogenes* inside infected cells. Cell Motil. Cytoskelet. **28:**97–107.
11. **Domann, E., J. Wehland, M. Rohde, S. Pistor, M. Hartl, W. Goebel, M. Leimeister-Wachter, M. Wuenscher, and T. Chakraborty.** 1992. A novel bacterial virulence gene in *Listeria monocytogenes* required for host cell microfilament interaction with homology to the proline-rich region of vinculin. EMBO J. **11:**1981–1990.
12. **Geiger, B.** 1979. A 130K protein from chicken gizzard: its localization at the termini of microfilament bundles in cultured chicken cells. Cell **18:**193–205.
13. **Goldberg, M. B., O. Bârzu, C. Parsot, and P. J. Sansonetti.** 1993. Unipolar localization and ATPase activity of IcsA, a *Shigella flexneri* protein involved in intracellular movement. J. Bacteriol. **175:**2189–2196.
14. **Goldberg, M. B., and J. A. Theriot.** 1995. *Shigella flexneri* surface protein IcsA is sufficient to direct actin-based motility. Proc. Natl. Acad. Sci. USA **92:**6572–6576.
15. **Goldstein, L., R. Rubin, and C. Ko.** 1977. The presence of actin in nuclei: a critical appraisal. Cell **12:**601–608.
16. **Hackstadt, T., R. Messer, W. Cieplak, and M. G. Peacock.** 1992. Evidence for proteolytic cleavage of the 120-kilodalton outer membrane protein of rickettsiae: identification of an avirulent mutant deficient in processing. Infect. Immun. **60:**159–165.

16a. **Heinzen, R. A.** Unpublished observations.
17. **Heinzen, R. A., S. F. Hayes, M. G. Peacock, and T. Hackstadt.** 1993. Directional actin polymerization associated with spotted fever group rickettsia infection of Vero cells. Infect. Immun. **61:**1926–1935.
18. **Kocks, C., E. Gouin, M. Tabouret, P. Berche, H. Ohayon, and P. Cossart.** 1992. *L. monocytogenes*-induced actin assembly requires the *actA* gene product, a surface protein. Cell **68:**521–531.
19. **Kocks, C., R. Hellio, P. Gounon, H. Ohayon, and P. Cossart.** 1993. Polarized distribution of *Listeria monocytogenes* surface protein ActA at the site of directional actin assembly. J. Cell Sci. **105:**699–710.
20. **Kocks, C., J. B. Marchand, E. Gouin, H. d'Hauteville, P. J. Sansonetti, M. F. Carlier, and P. Cossart.** 1995. The unrelated surface proteins ActA of *Listeria monocytogenes* and IcsA of *Shigella flexneri* are sufficient to confer actin-based motility on *Listeria innocua* and *Escherichia coli*, respectively. Mol. Microbiol. **18:**413–423.
21. **Laine, R. O., W. Zeile, F. Kang, D. L. Purich, and F. S. Southwick.** 1997. Vinculin proteolysis unmasks an ActA homolog for actin-based *Shigella* motility. J. Cell Biol. **138:**1255–1264.
22. **Lasa, I., V. David, E. Gouin, J. B. Marchand, and P. Cossart.** 1995. The amino-terminal part of ActA is critical for the actin-based motility of *Listeria monocytogenes*; the central proline-rich region acts as a stimulator. Mol. Microbiol. **18:**425–436.
23. **Lett, M. C., C. Sasakawa, N. Okada, T. Sakai, S. Makino, M. Yamada, K. Komatsu, and M. Yoshikawa.** 1989. *virG*, a plasmid-coded virulence gene of *Shigella flexneri*: identification of the *virG* protein and determination of the complete coding sequence. J. Bacteriol. **171:**353–359.
24. **Ludin, B., and A. Matus.** 1998. GFP illuminates the cytoskeleton. Trends Cell Biol. **8:**72–77.
25. **Maciver, S. K.** 1998. How ADF/cofilin depolymerizes actin filaments. Curr. Opin. Cell Biol. **10:**140–144.
26. **Miki, H., T. Sasaki, Y. Takai, and T. Takenawa.** 1998. Induction of filopodium formation by a WASP-related actin-depolymerizing protein N-WASP. Nature **391:**93–96.
27. **Monderloh, U. G., S. F. Hayes, J. Cummings, and T. J. Kurtti.** 1998. Microscopy of spotted fever rickettsia movement through tick cells. Microsc. Microanal. **4:**115–121.
28. **Niebuhr, K., F. Ebel, R. Frank, M. Reinhard, E. Domann, U. D. Carl, U. Walter, F. B. Gertler, J. Wehland, and T. Chakraborty.** 1997. A novel proline-rich motif present in ActA of *Listeria monocytogenes* and cytoskeletal proteins is the ligand for the EVH1 domain, a protein module present in the Ena/VASP family. EMBO J. **16:**5433–5444.
29. **Pante, N., and U. Aebi.** 1993. The nuclear pore complex. J. Cell Biol. **122:** 977–984.
30. **Peterson, J. L., and E. H. McConkey.** 1976. Non-histone chromosomal proteins from HeLa cells. A survey by high resolution, two-dimensional electrophoresis. J. Biol. Chem. **251:**548–554.
31. **Prévost, M. C., M. Lesourd, M. Arpin, F. Vernel, J. Mounier, R. Hellio, and P. J. Sansonetti.** 1992. Unipolar reorganization of F-actin layer at bacterial division and bundling of actin filaments by plastin correlate with movement of *Shigella flexneri* within HeLa cells. Infect. Immun. **60:**4088–4099.
32. **Pring, M., A. Weber, and M. R. Bubb.** 1992. Profilin-actin complexes directly elongate actin filaments at the barbed end. Biochemistry **31:**1827–1836.
33. **Reinhard, M., K. Giehl, K. Abel, C. Haffner, T. Jarchau, V. Hoppe, B. M. Jockusch, and U. Walter.** 1995. The proline-rich focal adhesion and microfilament protein VASP is a ligand for profilins. EMBO J. **14:**1583–1589.
34. **Reinhard, M., M. Rudiger, B. M. Jockusch, and U. Walter.** 1996. VASP interaction with vinculin: a recurring theme of interactions with proline-rich motifs. FEBS Lett. **399:**103–107.
35. **Rosenblatt, J., B. J. Agnew, H. Abe, J. R. Bamburg, and T. J. Mitchison.** 1997. *Xenopus* actin depolymerizing factor/cofilin (XAC) is responsible for the turnover of actin filaments in *Listeria monocytogenes* tails. J. Cell Biol. **136:**1323–1332.
36. **Sanger, J. M., J. W. Sanger, and F. S. Southwick.** 1992. Host cell actin assembly is necessary and likely to provide the propulsive force for intracellular movement of *Listeria monocytogenes*. Infect. Immun. **60:**3609–3619.
37. **Smith, G. A., D. A. Portnoy, and J. A. Theriot.** 1995. Asymmetric distribution of the *Listeria monocytogenes* ActA protein is required and sufficient to direct actin-based motility. Mol. Microbiol. **17:**945–951.
38. **Smith, G. A., J. A. Theriot, and D. A. Portnoy.** 1996. The tandem repeat domain in the *Listeria monocytogenes* ActA protein controls the rate of actin-based motility, the percentage of moving bacteria, and the localization of vasodilator-stimulated phosphoprotein and profilin. J. Cell Biol. **135:**647–660.
39. **Stochaj, U., and P. Silver.** 1992. Nucleocytoplasmic traffic of proteins. Eur. J. Cell Biol. **59:**1–11.
40. **Suzuki, T., H. Miki, T. Takenawa, and C. Sasakawa.** 1998. Neural Wiskott-Aldrich syndrome protein is implicated in the actin-based motility of *Shigella flexneri*. EMBO J. **17:**2767–2776.
41. **Suzuki, T., S. Saga, and C. Sasakawa.** 1996. Functional analysis of *Shigella* VirG domains essential for interaction with vinculin and actin-based motility. J. Biol. Chem. **271:**21878–21885.
42. **Teyssiere, N., C. Chiche-Portiche, and D. Raoult.** 1992. Intracellular movements of *Rickettsia conorii* and *R. typhi* based on actin polymerization. Res. Microbiol. **143:**821–829.
43. **Theriot, J. A.** 1995. The cell biology of infection by intracellular bacterial pathogens. Annu. Rev. Cell Dev. Biol. **11:**213–239.
44. **Theriot, J. A., T. J. Mitchison, L. G. Tilney, and D. A. Portnoy.** 1992. The rate of actin-based motility of intracellular *Listeria monocytogenes* equals the rate of actin polymerization. Nature **357:**257–260.
45. **Theriot, J. A., J. Rosenblatt, D. A. Portnoy, P. J. Goldschmidt-Clermont, and T. J. Mitchison.** 1994. Involvement of profilin in the actin-based motility of *L. monocytogenes* in cells and in cell-free extracts. Cell **76:**505–517.
46. **Tilney, L. G., and D. A. Portnoy.** 1989. Actin filaments and the growth, movement, and spread of the intracellular bacterial parasite, *Listeria monocytogenes*. J. Cell Biol. **109:**1597–1608.
47. **Todd, W. J., W. Burgdorfer, A. J. Mauros, and G. P. Gray.** 1981. Ultrastructural analysis of *Rickettsia rickettsii* in cultures of persistently infected vole cells, p. 248–250. *In* W. Burgdorfer and R. L. Anacker (ed.), Rickettsiae and rickettsial diseases. Academic Press, Inc., New York, N.Y.
48. **Welch, M. D., A. H. DePace, S. Verma, A. Iwamatsu, and T. J. Mitchison.** 1997. The human Arp2/3 complex is composed of evolutionarily conserved subunits and is localized to cellular regions of dynamic actin filament assembly. J. Cell Biol. **138:**375–384.
49. **Welch, M. D., A. Iwamatsu, and T. J. Mitchison.** 1997. Actin polymerization is induced by Arp2/3 protein complex at the surface of *Listeria monocytogenes*. Nature **385:**265–269.
50. **Welch, M. D., J. Rosenblatt, J. Skoble, D. A. Portnoy, and T. J. Mitchison.** 1998. Interaction of human Arp2/3 complex and the *Listeria monocytogenes* ActA protein in actin filament nucleation. Science **281:**105–108.
51. **Winkler, H. H.** 1990. *Rickettsia* species (as organisms). Annu. Rev. Microbiol. **44:**131–153.

Editor: P. E. Orndorff